Polyanionic Hydrogels as Reservoirs for Polycationic Antibiotic Substitutes Providing Prolonged Antibacterial Activity

Varvara Gribova, Fouzia Boulmedais, Agnès Dupret-Bories, Cynthia Calligaro, Bernard Senger, Nihal Engin Vrana, and Philippe Lavalle*

ABSTRACT: Implantation of biomedical devices is often followed by bacterial infections that may seriously affect implant functionalities and lead to their failure. In the context of bacterial resistance to antibiotics, which is a growing problem worldwide, new strategies that are able to overcome these problems are needed. In this work, we introduce a new formulation of hyaluronic acid (HA)-based antimicrobial material: HA hydrogels loaded with polyarginine (PAR), a polycationic antibiotic substitute. The loading is possible through electrostatic interactions between negatively charged HA and positively charged PAR. Such hydrogels absorb high quantities of PAR, which are then gradually released from the hydrogel. This original system provides a long-lasting antibacterial effect on an in vitro model of repetitive infection, thus demonstrating a strong potential to fight multiple rounds of infections that are resistant to antibiotic treatment. In addition, HA-PAR hydrogels could be deposited onto/into medical devices such as wound dressings and mesh prostheses used in clinical applications. Finally, we performed first in vivo tests of hydrogel-coated mesh materials to verify their biocompatibility in a rat model, which show no difference between control HA hydrogel and PAR-loaded hydrogel in terms of inflammation.

KEYWORDS: antibiotic substitute, hydrogel, hyaluronic acid, polyarginine, implants, mesh
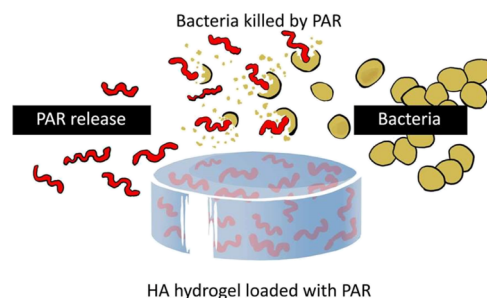
■ INTRODUCTION

Implantation of medical devices is often followed by bacterial infections that may seriously affect implant functionalities and even lead to their failure.[1] The rate of medical device-related infections varies from 5−8% for central venous catheters to 25−50% for heart-assist devices.[2] These infections are mostly induced by *Staphylococcus epidermidis*, *Pseudomonas aeruginosa*, *Staphylococcus aureus*, and enterobacteria such as *Escherichia coli*.[3] The bacteria adhere to materials that promote formation of biofilms, which are composed of bacteria in a hydrated polymeric matrix of their own synthesis.[4,5]

Conservative approaches to prevent or fight the infection include using of antibiotics (locally or systemically) and antiseptics (locally).[6] New approaches such as materials containing antibiotics that are applied locally during the surgery are being developed. One of the approaches to fight the infection locally consists in using antibiotic-loaded collagen sponges that are now widely used for different clinical applications.[7−9] For instance, Musella et al. described insertion of a gentamicin-treated collagen tampon adjacent to a polypropylene (PP) mesh used for repairing groin hernias, which is reduced by > 6-fold the rate of wound infections.[7] More recently, hyaluronic acid (HA) hydrogel coatings to protect implanted biomaterials in orthopedics, trauma, and maxillofacial surgery were developed. Such hydrogels can be loaded with antibiotics and applied to the implant surface at the time of surgery.[10] Currently, new antibiotic-releasing systems are being developed, for instance, a pH-responsive hydrogel obtained by reacting oxidized dextran with aminoglycoside and an ornidazole has been recently described.[11]

However, bacteria resistance to antibiotics is a growing problem worldwide.[12] Hence, antimicrobial agents, which are able to overcome antibiotic resistance problem, are needed. One of the most common antimicrobial agent family is based on metals such as silver, gold, copper, and zinc.[13] They can be used as surface coating or embedded into hydrogels as nanoparticles. However, there remains uncertainties about safety of metallic nanoparticles such as silver as they have potential secondary effects and elevated cytotoxicity at high concentrations.[14] Antimicrobial peptides (AMPs) are another category of emerging therapeutic agents.[15] Despite recent progress, scale-up in their production remains a main challenge. Other molecules/substances recently used as antibiotic substitutes include pyrrolidinium ionic liquids,[16] polyhexamethylene guanidine phosphate,[17] hinokitiol,[18] and

curcumin.[19] The exhaustive list of antibiotic substitutes used to functionalize the hydrogels can be found in specialized reviews.[20−22]

Polyarginine (PAR) is a polycationic polypeptide presenting antimicrobial activity in solution, with minimum inhibitory concentration (MIC) depending on the PAR length.[23] It can be produced by polymerization that makes PAR more profitable compared to AMPs. We have previously described thin films made of PAR and HA, constructed by layer-by-layer assembly,[24] which demonstrated antimicrobial and anti-inflammatory properties.[23,25,26] Interestingly, antimicrobial activity of PAR-containing layer-by-layer films was only observed for PAR of 30 arginine residues (PAR30). Moreover, this activity was demonstrated only when PAR30 was associated to HA and did not work for other polyanions (e.g., alginate). This property is probably related to the strong diffusion capacity of PAR30 chains in (PAR30/HA) multi-layers compared to their diffusion ability in the other films.[26]

HA is a polyanionic polysaccharide composed of a repeating disaccharide unit of (1,4)-glucuronic acid-β (1,3)-N-acetylglu-cosamine (GlcNAc), and it is naturally present in the extracellular matrix of vertebrate tissues.[27,28] Synovial fluid, vitreous humor of the eye, and hyaline cartilage are especially rich in HA. HA is known to promote wound healing, is biocompatible, and already used for multiple biomedical applications such as dermal injections, osteoarthritis treatment, eye surgery, and wound regeneration.[29] HA is also known to have antifouling properties, which reduces bacterial adhe-sion.[30−32] In one study, HA was grafted with AMP nisin in order to elaborate an antimicrobial biopolymer combining properties of nisin and HA.[33]

Another advantage of HA is the possibility to form hydrogels with tunable properties via cross-linking, which allows to adapt them to a given application and control HA degradation rate.[34] Among different cross-linkers, BDDE (1,4-butanediol digly-cidyl ether) is by far the most commonly employed nowadays, for example, it is used in the production of majority of dermal fillers for esthetic purposes.[35,36] The advantage of BDDE as a cross-linking agent is that at high pH, it cross-links via hydroxyl groups,[36] while leaving negatively charged carboxyl groups available for complexation with positively charged molecules, for instance, with PAR.

In this work, we introduce a new formulation of HA-based antimicrobial material: HA hydrogels cross-linked with BDDE and loaded with PAR. We demonstrate that HA hydrogels can be loaded with PAR of different lengths, and some conditions provide a long-lasting antibacterial effect because of a gradual release of PAR from the hydrogel. Thus, they could be potentially used to fight persistent infections that are difficult to eradicate.[37]

The hydrogels were also deposited onto medical devices such as wound dressings and mesh prostheses used for hernia repair. Deposition of the HA-PAR hydrogels onto these materials is simple and shows efficient antimicrobial properties. This represents an important step because meshes used for hernia repair present a high risk of postoperative infection. For instance, up to 8% of up to 8% of ventral hernial repairs by meshes become infected and may require excision.[38]

Antibacterial HA-PAR hydrogels, alone or deposited on medical devices, can be used in the future to treat infected wounds, prevent infections related to implantation, and eradicate persistent infections because of PAR gradual release.

■ MATERIALS AND METHODS

Materials. Poly(L-arginine hydrochloride) (PAR) was purchased from Alamanda Polymers, USA. The different PAR polymers used differ by the numbers of arginine residues per chain: PAR10 (MW = 1.9 kDa), PAR30 (MW = 5.8 kDa), and PAR200 (MW = 38.5 kDa). HA (MW = 823 kDa) used as the polyanion was purchased from Lifecore Biomed (USA). Tris(hydroxymethyl)-aminomethane (Tris), butanediol diglycidyl ether (BDDE), thiazolyl blue tetrazolium bromide (MTT), and Mueller Hinton (MH) broth medium were purchased from Merck (Germany). DMEM (Dulbecco's modified Eagle medium) and 100× penicillin−streptomycin were purchased from Dominique Dutscher (France), and fetal bovine serum (FBS) was purchased from Gibco/ThermoFicher Scientific (France). Gynecare Gynemesh PS (Ethicon, USA) was kindly provided by Dr Nicolas Sananes.

Preparation of HA Hydrogels. To prepare HA hydrogels, 1.5 mL of 2.5% HA (MW = 823 kDa) solution in NaOH (0.25 M) was mixed with 20% BDDE (v/v) and poured into a 35 mm diameter Petri dish. The mixture was allowed to cross-link at room temperature for 72 h (Figure 1A). The hydrogel was further cut, most of the time,
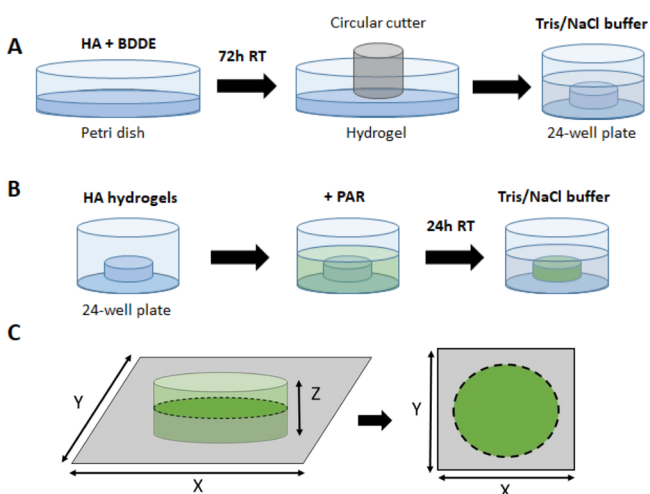

Figure 1. Preparation of HA-PAR hydrogel discs. (A) Production of HA hydrogel discs: HA (1.5 mL) and BDDE well-mixed solution is poured into a Petri dish and allowed to cross-link at room temperature for 72 h. The hydrogel was further cut into the discs of required size using a circle cutter. (B) HA hydrogel discs loading with PAR for 24 h, followed by rinsing in Tris/NaCl buffer. (C) Confocal microscopy imaging of hydrogel discs.

into 4 mm discs using a circle cutter, and rinsed in Tris 10 mM/NaCl 0.15 M buffer (further referred to as Tris/NaCl buffer). One fast 1 min rinsing and a longer 1 h rinsing were performed. After this procedure, 4 mm diameter discs have swollen and became 6 mm diameter discs. Initially, HA of several molecular weights, as well as different concentrations of both HA and BDDE, was tested. Conditions allowing formation of a free-standing, handable optimal gel were finally selected and are now described in this study.

Rheological Characterization of HA Hydrogels. Rheological measurements were performed in HA−BDDE mixture using a Kinexus rheometer and d = 40 mm cone geometry. Briefly, 1.2 mL of freshly mixed HA−BDDE solution was deposited between the cone and the plate, and gelation was followed at 25 °C for 72 h at a frequency of 1 Hz. To avoid evaporation, the solvent trap was used.

Loading and Release of PAR. To load PAR into the hydrogels, the discs were immersed in PAR solution in Tris/NaCl buffer and incubated for 24 h at room temperature on a moving plate (Figure 1B). For 6 mm discs in the 24-well plate, 0.5 mL of PAR solution was used. After incubation, the discs were rinsed with Tris/NaCl buffer (one quick and one long rinsing, 5 min and 1 h, respectively).

For PAR release experiments, discs loaded with fluorescein isothiocyanate-conjugated PAR (PAR-FITC, produced in the laboratory as described previously[23]) were incubated at 37 °C with respective solution (NaCl 1 M, MH medium or DMEM supplemented with 10% FBS and 1% antibiotics). The release quantification of PAR-FITC in solution was performed by measuring the fluorescence of the supernatant with a spectrofluorimeter (SAFAS Xenius XC spectrofluorimeter, Monaco) with an excitation/emission wavelength of 488/517 nm.

Confocal laser scanning microscopy (CSLM, LSM 710 microscope, Zeiss, Heidelberg, Germany) was also used to characterize PAR loading and release. To characterize PAR loading, the discs were incubated with PAR-FITC as described above, and then disc $X \times Y$ cross-cut images were taken in the middle of the discs (Figure 1C).

Fourier-Transform Infrared Spectroscopy. Fourier-transform infrared spectroscopy (FTIR) experiments were performed on a Vertex 70 spectrometer (Bruker, Germany) using a DTGS detector. Spectra were recorded in the Attenuated total reflection (ATR) mode using single reflection diamond ATR by averaging 128 interferograms between 600 and 4000 cm^{-1} at 2 cm^{-1} resolution using Blackman–Harris three-term apodization and Bruker OPUS/IR software (version 7.5). HA gels were prepared in deuterated solution using the standard protocol, incubated in Tris/NaCl deuterated solution in the absence or the presence of 1 mg·mL^{-1} PAR and dried before the measurement. The normalization was performed on the entire spectra recorded between 800 and 4000 cm^{-1} by applying the min/max normalization of OPUS 7.5 software. This normalization allows to compare spectra with each other when the optical layer thickness substantially varies. As the diffusion of PAR inside HA gel leads to its contraction, FTIR spectra of HA/PAR gels have higher intensities in comparison to the HA gel because of the probing of more material on the surface. Thus, the normalization of FTIR spectra was applied by attributing to the highest peak of the HA with the value of 1. This normalization allows the comparison of the spectra for the same quantity of HA probed by the IR source. As in each sample, the polysaccharide peaks have the highest intensity, and the normalization is obtained toward the quantity of HA probed by the IR source.

Fluorescence Recovery after Photobleaching Experiments. Fluorescence recovery after photobleaching (FRAP) experiments were performed on HA hydrogels incubated with 0.5 mg·mL^{-1} of fluorescently labeled PAR and immersed in Tris/NaCl buffer. One circular region (95 μm in radius in an image of 850 μm × 850 μm) was exposed for 64.4 s to the light of a laser set at its maximum power (λ = 488 nm). Then, the recovery of fluorescence in the bleached area was followed over time. Observations were carried out with the confocal microscope using a 10× objective. At the same time, four equally sized circular reference areas outside of the bleached area were monitored. The intensities in these areas were used to normalize the intensity in the bleached area, so that bleaching because of image acquisition was accounted for.

Antibacterial Assays. S. aureus (ATCC 25923), E. coli (ATCC 25922), and P. aeruginosa (ATCC 27853) strains were used to assess the antibacterial properties of the test samples. Bacteria were precultured aerobically at 37 °C in a MH broth medium, pH 7.3. For this, one colony from the previously prepared agar plate with streaked bacteria was transferred to 10 mL of MH medium and incubated at 37 °C. Overnight culture was adjusted to OD$_{620nm}$ = 0.001 (approximately 8 × 10^5 CFU.mL^{-1}) by diluting in MH and added to the wells of a 24-well plate containing d = 6 mm HA hydrogels loaded with different concentrations of PAR and sterilized with UV for 15 min. Antibacterial effect of HA-PAR hydrogels was quantified by measuring OD$_{620nm}$ after 24 h of incubation at 37 °C on a moving plate (Figure S1). In repetitive culture experiments, bacterial suspension (OD$_{620nm}$ = 0.001) was replaced every 24 h.

In Vitro Cytotoxicity Tests. The Balb/3T3 (ATCC CCL163) mouse embryonic fibroblast cell line was cultured at 37 °C in DMEM with 10% of FBS and 1% of penicillin−streptomycin (further referred to as "DMEM"). The cytotoxicity tests were performed according to ISO 10993-5. For the direct cytotoxicity test, we used 4 mm diameter discs, which swell and become ∼6 mm diameter when placed in Tris/

NaCl buffer. The discs, loaded or not with PAR, were sterilized with UV for 15 min and placed onto ∼80% confluent layer of BALB/3T3 cells (passage 2 to 15) cultured in a 24-well plate (Figure S2). After 24 or 48 h at 37 °C, phase contrast images were taken around and under the discs to evaluate the cell morphology. The images were captured using an Olympus CDX41 microscope (Olympus Corporation, Japan) with an Infinity 2 camera and Infinity Analyze software. Then, hydrogel discs were removed, and MTT test was performed in order to measure cell metabolic activity. For MTT assay, the cells were incubated for 3 h in 0.2 mg·mL^{-1} MTT-containing cell culture medium. The medium was then removed, and formazan was dissolved in dimethyl sulfoxide (0.5 mL per well of a 24-well plate). Absorbance of resulting solutions was measured at 570 nm using the spectrophotometer.

Hydrogel Deposition onto Nonwoven/mesh Materials. To deposit the hydrogels onto materials (Medicomp, a nonwoven fabric used for wounds disinfection and GYNECARE GYNEMESH PS Nonabsorbable PROLENE Soft Mesh), HA−BDDE solution (50 μL) was deposited on 12 mm diameter fabric or mesh piece and allowed to cross-link as previously described.

In Vivo Biocompatibility. Ten 8-week-old male Wistar rats (300−400 g in weight), provided by a certified breeding center (Charles River, France), were used for this study. The animals were received at the CREFRE (US 006/CREFRE-Inserm/UPS/ENVT) animal supplier (no. A31555010 issued December 17, 2015). Protocols were submitted to the CREFRE ethics committee with approval, in accordance with the European directive (DE 86/609/CEE; modified DE 2003/65/CE) for conducting animal experiments. One week of acclimatization was respected. The animals were housed in ventilated cages with a double level (two animals per cage according to European standards). The animals were carefully monitored (behavior and food intake) and were weighed weekly throughout the experiment. The 10 rats received each two round implants (diameter of 1 cm), one implant on left side and one implant on right side. In total, there were five implantations of dried and autoclaved hydrogels deposited onto mesh materials for each of the following conditions: (i) HA-only hydrogels; (ii) HA hydrogels loaded with PAR10 at 0.1 mg·mL^{-1}; (iii) HA hydrogels loaded with PAR30 at 0.05 mg·mL^{-1}; (iv) HA hydrogels loaded with PAR30 at 0.1 mg·mL^{-1}.

The rats were induced by isoflurane 4% and maintenance of 2%. Each rat was placed in a prone position on a heated pad. After shaving and scrubbing with betadine, two 20 mm dorsal incisions were made over the thoracolumbar area, one on the right side and one on the left side. One scaffold was inserted at both sides into subcutaneous pockets. All the incisions were closed with Vicryl 3-0. All rats received buprenorphine (0.6 mg/kg) injected subcutaneously twice per day for 5 days. All animals survived the duration of the study with no adverse effects. Euthanasia were performed after 14 days. The animals were first anesthetized with the isoflurane device and masked and then slowly injected with an overdose of pentobarbital (150 mg/kg) in the intraperitoneal route. After the expiration of the animal death, the implants with surrounding tissue were explanted and collected to perform histology.

For histological analysis, the samples were fixed in 4% formalin. Macroscopic sections were embedded in paraffin. Five micrometer thick sections were stained with hematoxylin−eosin−saffron. For each sample, microscopic optical analysis was realized with software NDP.view2 (Hamamatsu, Massy, France) after slides scanning (NanoZoomer, Hamamatsu) with the following criteria: semi-quantitative assessment of acute inflammation, chronic inflammation, fibroblastic reaction, edema, fibrosis, angiogenesis, and periprosthetic histiocytic reaction.

Statistical Analysis. Rheology, loading/release, FRAP, antibacterial assays, and cytotoxicity test experiments were performed at least three times. Either representative results or averages from three independent experiments are shown in the figures. The data were processed by using SigmaPlot (Systat Software Inc., USA). One-way ANOVA on the Ranks test was performed to evaluate statistical significance in the cytotoxicity assay.

RESULTS AND DISCUSSION

HA Hydrogel Formation and Disc Model. HA hydrogel gelation kinetics is followed in Figure 2A through macroscopic
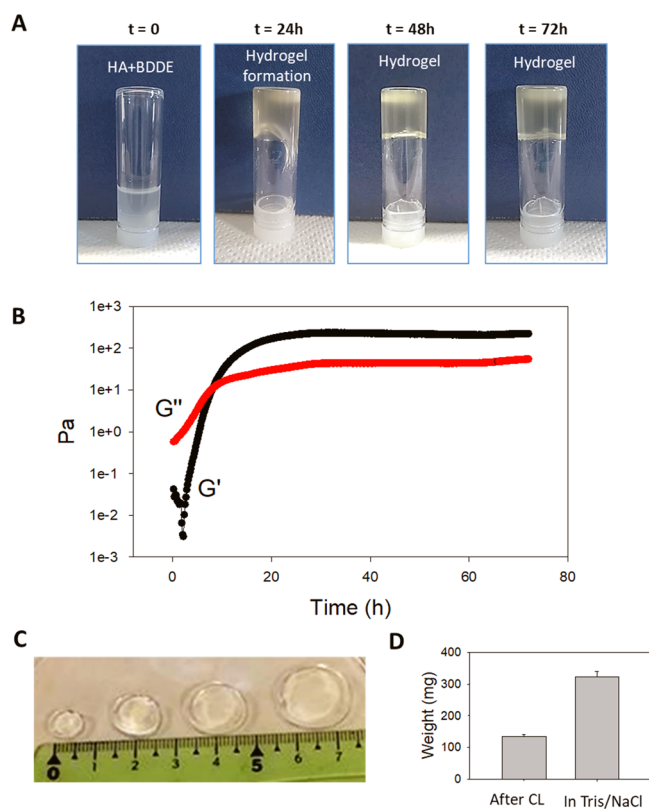

Figure 2. HA hydrogel preparation and characterization. (A) Monitoring of the HA gelation when BDDE is added to produce the hydrogel. (B) Rheological characterization of HA-BDDE hydrogel formation by monitoring elastic and viscous moduli as a function of time. Gelation was followed at 25 °C for 72 h at a frequency of 1 Hz. The experiment was repeated three times. (C) Production of hydrogel discs of different sizes. (D) Hydrogel in NaOH 0.25 M (d = 18 mm after cutting) swelling in Tris/NaCl buffer.

observations. At 24 h, the gelation is starting, and after 48 h, the hydrogel is in place. These qualitative observations were confirmed by rheological monitoring of changes in viscoelastic properties over time (Figure 2B). According to the graph, about 40 h was required to reach a plateau. For commodity reasons, the hydrogels were cross-linked for 72 h (over a weekend) before being cut to discs of different sizes (Figure 2C). Then, after rinsing and incubation in Tris/NaCl buffer, the gels swelled about two times (weight) (Figure 2D). For experiments in 24-well plates, 6 mm diameter and ~1 mm height discs were used.

PAR Loading and Release from HA Hydrogels. To study loading of PAR in the hydrogels, PAR of three different chain lengths were used: PAR10, PAR30, and PAR200 (10, 30 and 200 arginine residues, respectively). For loading, hydrogels were incubated with PAR solutions prepared in Tris/NaCl buffer for 24 h. Shorter loading time (3 h) led to PAR loading on the disc periphery, while the center remained unloaded, as demonstrated with fluorescently labeled PAR (PAR-FITC) (Figure S3A,B).

PAR loading into HA hydrogels was also characterized by FTIR. The spectra (Figure S3C) show an amide I band at

1645 cm^{-1}, due to the carbonyl group of amide bonds of both HA and PAR, and saccharide peaks at 1040 and 1080 cm^{-1}, attributed to C−O bond stretching.[39,40] By comparing HA gels before and after incubation with PAR30 solutions, an increase of the amide I peak is observed with a shifting from 1614 to 1626 cm^{-1} because of the contribution of the amide I band of PAR. Moreover, an inversion of the intensities of the polysaccharide peaks was observed with PAR-loaded hydrogels. This is explained by the influence of the carboxylic group state of HA on the hydrogen bond network, as reported by Rinaudo and co-workers.[41] The presence of PAR led to a higher contribution of 1080 cm^{-1} in comparison to 1040 cm^{-1} as reported for HA in the acidic form. This is probably related to the electrostatic interactions between positively charged arginine moieties of PAR and negatively charged carboxylic groups of HA. This suggests, together with fluorescent observations of PAR loading (Figure S3A,B), that the loading of PAR in HA hydrogel was effective.

An example of a disc loaded with PAR30-FITC for 24 h is shown in Figure 3A,B, where the disc morphology is visualized by confocal microscopy. The disc is about 6 mm in diameter and 1 mm high, giving a volume of approximately 0.03 cm^3 or 30 μL and almost homogeneously loaded with PAR30-FITC,
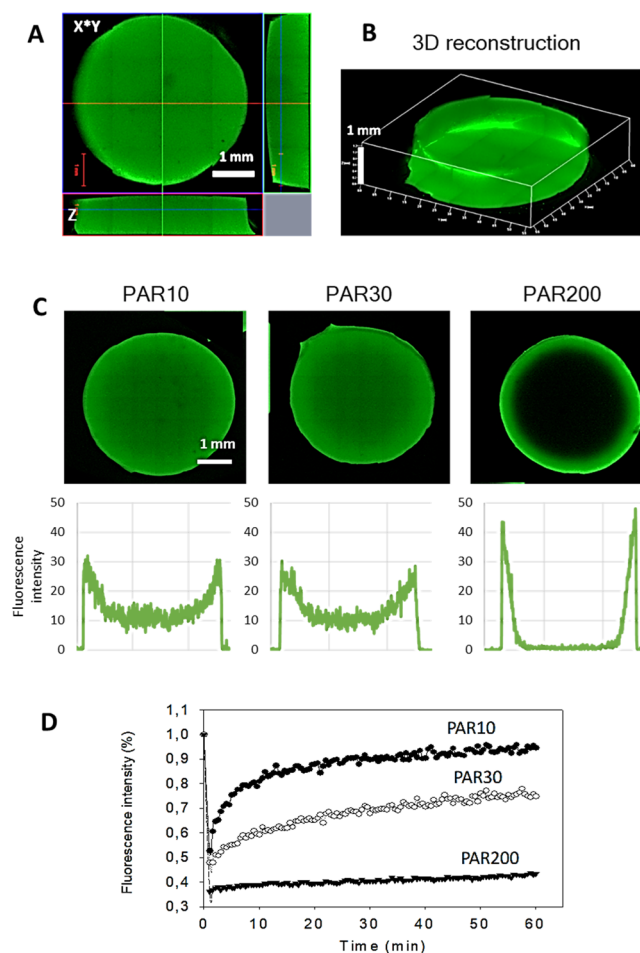

Figure 3. HA hydrogel loading with PAR. Confocal microscopy images of hydrogel discs incubated in 0.5 mg·mL^{-1} PAR30-FITC: cross-cuts in Z (A) and 3D reconstruction (B). (C) Confocal microscopy images and fluorescence intensity profiles of HA hydrogels incubated in 0.5 mg·mL^{-1} PAR10-FITC.

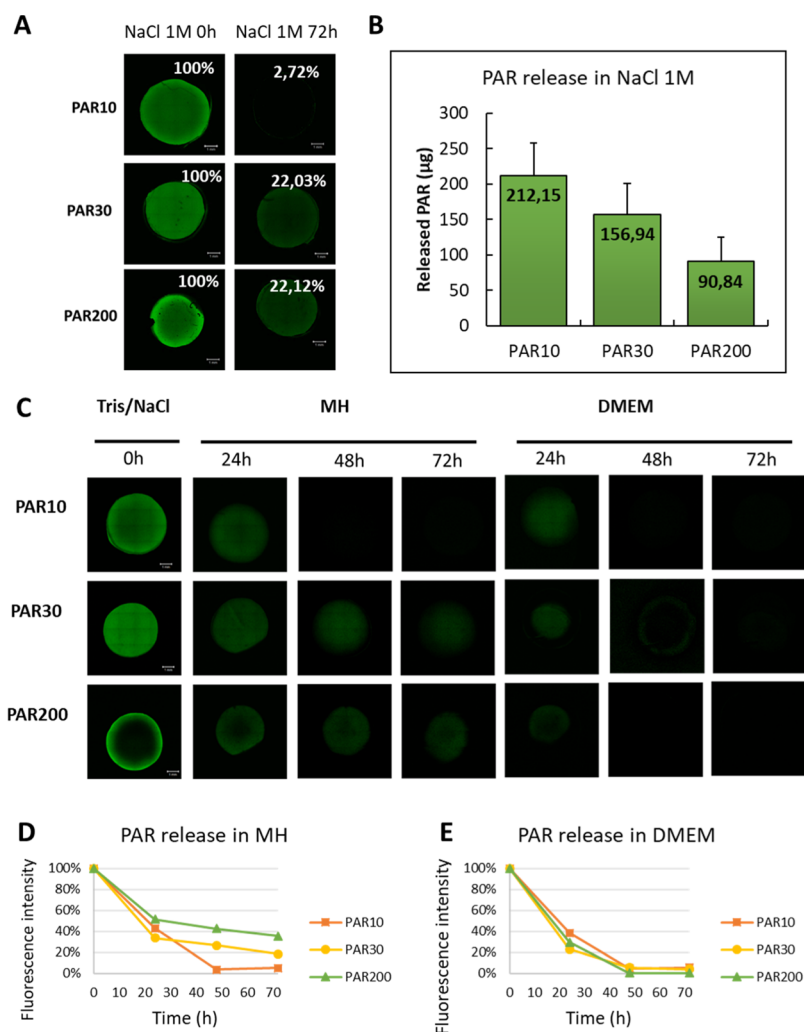**Figure 4.** Release of PAR in NaCl and in culture media. HA discs were incubated with 0.5 mg·mL^{-1} of three different FITC-conjugated PAR for 24 h. The discs were rinsed and then incubated for 72 h in NaCl 1 M, MH, or DMEM. (A) Confocal microscopy observations: percentage of PAR remaining after 72 h is indicated. (B) Quantification by spectrofluorimetry of PAR release after 72 h in NaCl 1 M. The graphs represent averages from three independent experiments, and error bars represent standard deviations. (C) Confocal microscopy images of the discs before and after incubation with MH and DMEM. (D) and (E) Percentage of released PAR in MH and DMEM, where 100% represent fluorescence intensity of the discs in Tris/NaCl.

although a higher fluorescence intensity on the disc periphery can be monitored.

Similar loading profile was observed for PAR10, while PAR200 chains mostly remained on the disc periphery and did not diffuse after 24 h to the center of the hydrogel (Figure 3C), which is in line with our previous observations, regarding the mobility of longer PAR chains in the PAR/HA polyelectrolyte multilayer:[23] PAR200 was less mobile, while PAR30 showed intermediate mobility and PAR10 being the most mobile, as determined by FRAP experiments for multilayer films. Similar conclusions can be drawn here from fluorescence recovery curves determined from FRAP measurements and performed with loaded hydrogels (Figure 3D).

Total amounts of PAR contained in the hydrogels were estimated by incubation of hydrogels loaded with fluorescently labeled PAR in concentrated NaCl to promote PAR release. After 72 h at 37 °C in NaCl 1 M, the release was almost complete for PAR10 and close to 80% for PAR30 and PAR200, according to the confocal microscopy images (Figure 4A). The percentage of PAR remaining in the hydrogel discs after 72 h of incubation was measured with image processing; 100%

corresponds to fluorescence intensity before release. Then, percentage of remaining PAR after NaCl 1 M incubation was determined to obtain a value of released PAR: about 97, 78, and 78% for PAR10, PAR30, and PAR200, respectively. Incomplete release of PAR30 and PAR200 correlates with lower mobility demonstrated by FRAP experiments (Figure 3D). Then, amounts of PAR-FITC released were quantified by measuring fluorescence intensity of the supernatant by spectrofluorimetry and referring to a calibration curve. The results show that the discs incubated in 0.5 mg·mL^{-1} PAR solutions released about 212 μg of PAR10-FITC, 157 μg of PAR30-FITC, and 91 μg of PAR200-FITC after 72 h in NaCl 1 M (Figure 4B). When correcting the released quantities to 100%, it gives 218, 201, and 117 μg of loaded PAR10-FITC, PAR30-FITC, and PAR200-FITC, respectively. Disc volume is approximately 30 μL, so the discs contain about 7.3 mg·mL^{-1} of PAR10, 6.7 mg·mL^{-1} of PAR30, and 3.9 mg·mL^{-1} of PAR200. Lower quantity of PAR200 in the hydrogels can be explained by its incomplete loading with most of PAR200 remaining on the disc periphery (Figure 3C).

PAR release from the hydrogels was then followed during 72 h in microbiological growth medium (MH) or cell culture medium (DMEM). PAR-FITC-loaded hydrogels were placed into these media and incubated at 37 °C, and PAR release was observed by confocal microscopy (Figure 4C). The release was faster for PAR10 in MH, compared to PAR30 and PAR200, which were released more gradually (Figure 4D). In DMEM, all three PAR had more or less similar release profiles and were completely released after 48 h (Figure 4E).

Antibacterial Activity of HA-PAR Hydrogels. After showing that HA hydrogels can be loaded with PAR, which is released in microbiological growth medium and cell culture medium, we tested antibacterial activity of HA-PAR hydrogel toward *S. aureus* as our model and because its presence is widely reported in implant-related nosocomial infections. At high-loading PAR concentrations (incubation in 1 mg·mL^{-1} PAR solutions), all three PAR inhibited *S. aureus* bacteria growth after 24 h (Figure S4). However, high concentration of loaded PAR might be toxic to the mammalian cells. To evaluate antibacterial properties of HA-PAR hydrogels in more details, we performed repetitive bacterial culture in the presence of HA hydrogel discs incubated in different concentrations of PAR. HA-PAR discs were incubated with bacterial suspension for 24 h, and then bacteria suspension was replaced every 24 h (Figure S1). This was done to mimic the worst conditions of repetitive bacterial infections, for example, in case of urinary or venous catheter-associated infections.

Hydrogels incubated in 0.05 mg·mL^{-1} of PAR10 and PAR30 solutions showed 1 and 2 days of antibacterial activity, respectively. Hydrogels incubated in 0.1 mg·mL^{-1} of PAR10 and PAR30 solutions showed 2 and 4 days of antibacterial activity, respectively. For higher PAR10 and PAR30 concentrations (incubation in 0.5 mg·mL^{-1} of PAR solutions), antibacterial activity lasted for 6 and 7 days, respectively (Figure 5A,B).

Interestingly, PAR10 loaded into HA hydrogel showed antibacterial effect, which was not the case in the PAR10/HA thin film, while in solution, all three PAR showed antibacterial activity.[23] However, antibacterial effect of PAR30 was more prolonged, compared to PAR10, which is probably because of slower release of PAR30 from the hydrogels. This correlates with PAR10 and PAR30 mobility inside the hydrogels (PAR10 being more mobile) (Figure 3D), and with release profiles (Figure 4D).

For hydrogels incubated in 0.5 mg·mL^{-1} PAR200 solution, some bacterial growth was already observed after 24 h, and the antimicrobial efficiency of the hydrogel decreased every following days (Figure 5C). Thus, PAR200 was much less efficient at equal w/v concentration when compared to PAR10 and PAR30. This can be because of its incomplete release from the hydrogels (Figure 4), in addition to its higher minimum inhibitory concentration (MIC) of 0.210 mg·mL^{-1}, as described previously.[23] MICs of PAR10 and PAR30 in solution (0.02 and 0.01 mg·mL^{-1}, respectively) combined with their higher released amounts can explain the high antibacterial activity of PAR10- and PAR30-loaded hydrogels.

According to Figure 4, about 218 μg of PAR10 was released after 72 h in NaCl. This quantity in a total volume of 0.4 mL of MH medium would correspond to a concentration of 0.545 mg·mL^{-1}, which is more than 20 times higher than MIC$_{10}$. For PAR30, 200 μg was released after 72 h in NaCl, corresponding to a concentration of 0.5 mg·mL^{-1}, which is almost 50 times higher than MIC$_{30}$. Thus, hydrogels contain enough PAR to
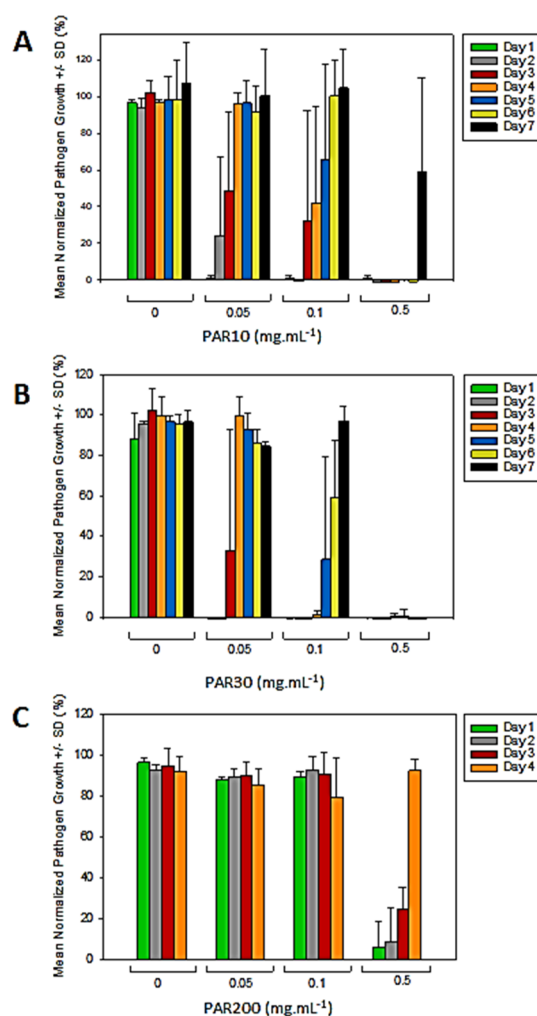

Figure 5. Antibacterial activity of HA hydrogels loaded with PAR10, PAR30, PAR200: repetitive culture. Every 24 h of bacterial culture, the samples were seeded with fresh bacteria. The graphs show bacterial growth in the presence of hydrogel discs loaded with PAR10 (A), PAR30 (B), and PAR200 (C). Data were normalized, and 100% corresponds to bacterial growth in the wells without hydrogels. The graphs represent averages from three independent experiments, and error bars represent standard deviations.

inhibit bacterial growth for several days. When PAR30 is released gradually, like in case of its release in MH (Figure 4C,D), it may provide, in theory, up to 40 days of antibacterial activity. In reality, after 72 h, 80% of PAR30 is released (Figure 4D). However, the remaining 20% correspond to approximately 40 μg of PAR30. If released into the medium (400 μL), it would give a concentration of 100 μg·mL^{-1}, which is 10 times higher than MIC. Thus, the remaining quantity is sufficient for several more days of antibacterial activity in MH medium. We have performed repetitive culture for up to 7 days, and no bacterial growth was observed for HA-PAR30 hydrogels incubated in 0.5 mg·mL^{-1} PAR30 solution.

Finally, we also tested if PAR30-loaded hydrogels can inhibit growth of other bacterial strains such as *E. coli* and *P. aeruginosa*, both Gram-negative bacteria which are responsible, together with Gram-positive *S. aureus*, of the majority of nosocomial infections. The antibacterial effect toward Gram-negative bacteria was observed at PAR30-loading concentrations equal to 0.1 mg·mL^{-1} and higher (Figure S5). For

loading concentrations of 0.5 and 1 mg·mL^{-1}, the antibacterial effect lasted for 3 days in the repetitive in vitro infection model.

Biocompatibility of HA-PAR Hydrogels. For use in clinical applications, antibacterial HA-PAR hydrogels have to be biocompatible. As a first step toward evaluation of HA-PAR hydrogel biocompatibility, we performed the in vitro direct cytotoxicity test (Figure S2), according to the ISO 10993-5 norm. Balb/3T3 fibroblasts were observed through microscopy after 24 h of incubation with hydrogel discs in DMEM medium, unloaded or loaded with 0.05 and 0.1 mg·mL^{-1} of PAR10 and PAR30, as well as 0.5 mg·mL^{-1} of PAR200. These concentrations correspond to the lowest antibacterial loading concentrations for each PAR (Figure 5). Confluent cell layers for the control, PAR10, and PAR30 (Figure 6A) were observed. However, in the condition where HA hydrogel was loaded with 0.5 mg·mL^{-1} PAR200, only rounded cells and cellular debris could be seen, suggesting cytotoxic effect of the aforementioned hydrogel.

These observations were confirmed by MTT test results: for unloaded hydrogels or those loaded with 0.05 and 0.1 mg·mL^{-1} of PAR10 and PAR30, cell viability was above 70% (100% corresponding to untreated cells), indicating the absence of cytotoxicity, according to ISO 10993-5 (Figure 6B). Condition in which the cells were incubated with 0.5 mg·mL^{-1} PAR200-loaded hydrogel showed decreased viability (43%) and was therefore considered as cytotoxic. PAR10- and PAR30-loading concentrations superior to 0.1 mg·mL^{-1} also showed cytotoxic response; however, these concentrations are significantly higher than the necessary concentration needed to provide robust antimicrobial activities (Figure S6).

According to Figure 4E, the total release of PAR in DMEM takes 48 h, therefore we checked cell viability after 24 and 48 h of incubation with HA-PAR hydrogels. The results showed that cell viability for PAR10 and PAR30-loaded hydrogels was similar or even higher after 48 h as compared to 24 h, with some viability decrease for PAR200 (Figure S7).

HA-PAR Hydrogel Deposition on Medical Devices. After demonstrating the antimicrobial activity of PAR-loaded HA hydrogels, we evaluated the possibility to associate them to medical materials used for clinical applications. We selected a nonwoven fabric used for wound cleaning and dressing (hydrophilic gauze made of 70% viscose and 30% polyester) and a polypropylene (PP) mesh used for treatment of urogynecological pathologies[42] (Figure 7A−C). HA hydrogels were successfully deposited onto both materials and showed antibacterial activity similar to HA hydrogel discs (Figure S8) after loading with PAR. Moreover, HA-PAR hydrogels deposited onto mesh prosthesis, dried, and sterilized by autoclaving, showed similar antibacterial activity as compared to nonsterilized samples (Figure 7D). Thus, HA-PAR hydrogels can be easily deposited onto wound cleaning/dressing materials to prevent or fight infection on the body surface but also integrated into implantable mesh materials to reduce the risk of implantation-related infection.

In Vivo Biocompatibility Assessment. Preliminary in vivo experiments were conducted on rats (10 animals). Each rat received two implants of hydrogel-coated meshes ($d = 1$ cm), one implant on the left side and one implant on the right side (Figure 7E). All animals survived the duration of the study with no adverse effects, and all animals gained weight in a normal way. After 14 days, the implants with the surrounding tissue were explanted and collected to perform histological analysis. An example of the histological sample is shown in Figure 7F. The results of the analysis showed the presence of inflammation in the tissues surrounding the implants (Figure S9 and Table S1). However, there was no difference between HA-only hydrogels and HA-PAR hydrogels, suggesting that PAR addition does not promote or increase inflammatory response. As described before, BDDE-crosslinked HA hydrogels are regularly used as the dermal filler, and if such a limited inflammation occurs, it has never been reported as being problematic. A future in vivo study confirming these results and including an infectious model should be planned to confirm the strong potential of this HA/PAR hydrogel for medical applications.
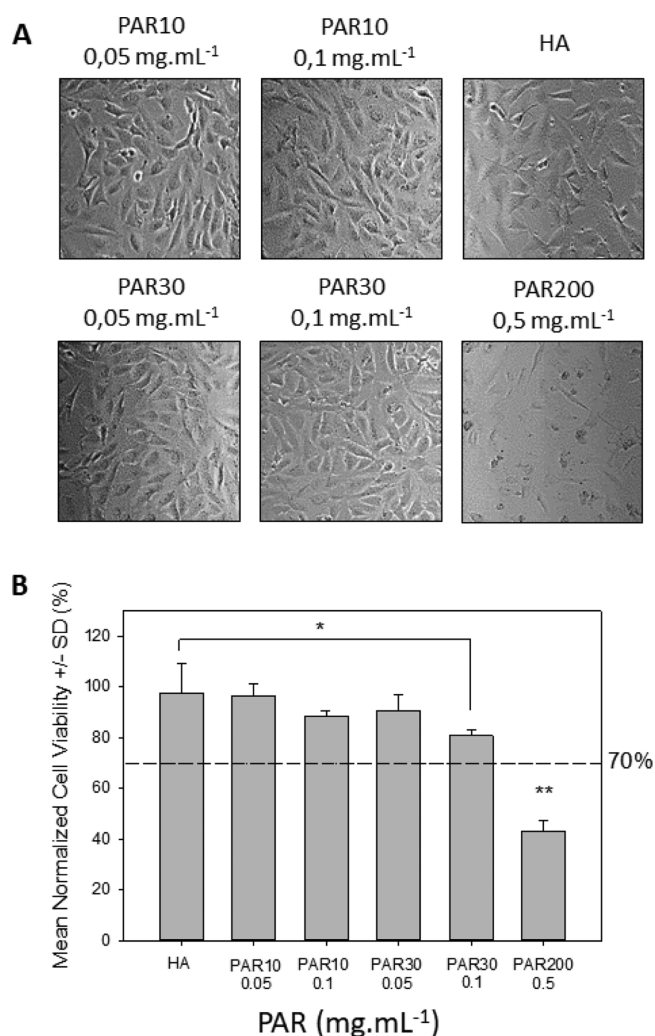

Figure 6. Cytotoxicity assay: Balb/3T3 cells are seeded in the 24-well plate and put in contact with HA hydrogel discs loaded or not with PAR for 24 h. "HA" corresponds to BDDE-crosslinked HA hydrogel discs without PAR, and other hydrogels were loaded with indicated PAR at different concentrations. (A) Cell morphology observed by phase contrast microscopy. (B) Cell viability evaluation by MTT test. Dotted line corresponds to 70% viability (cytotoxicity limit according to ISO standard 10993-5). The graphs represent averages from three independent experiments, and error bars represent standard deviations. *$p = 0.05$, **$p < 0.01$.

■ CONCLUSIONS

Because of the growing antibiotic resistance, new antibacterial agents are required, as well as new materials that can be
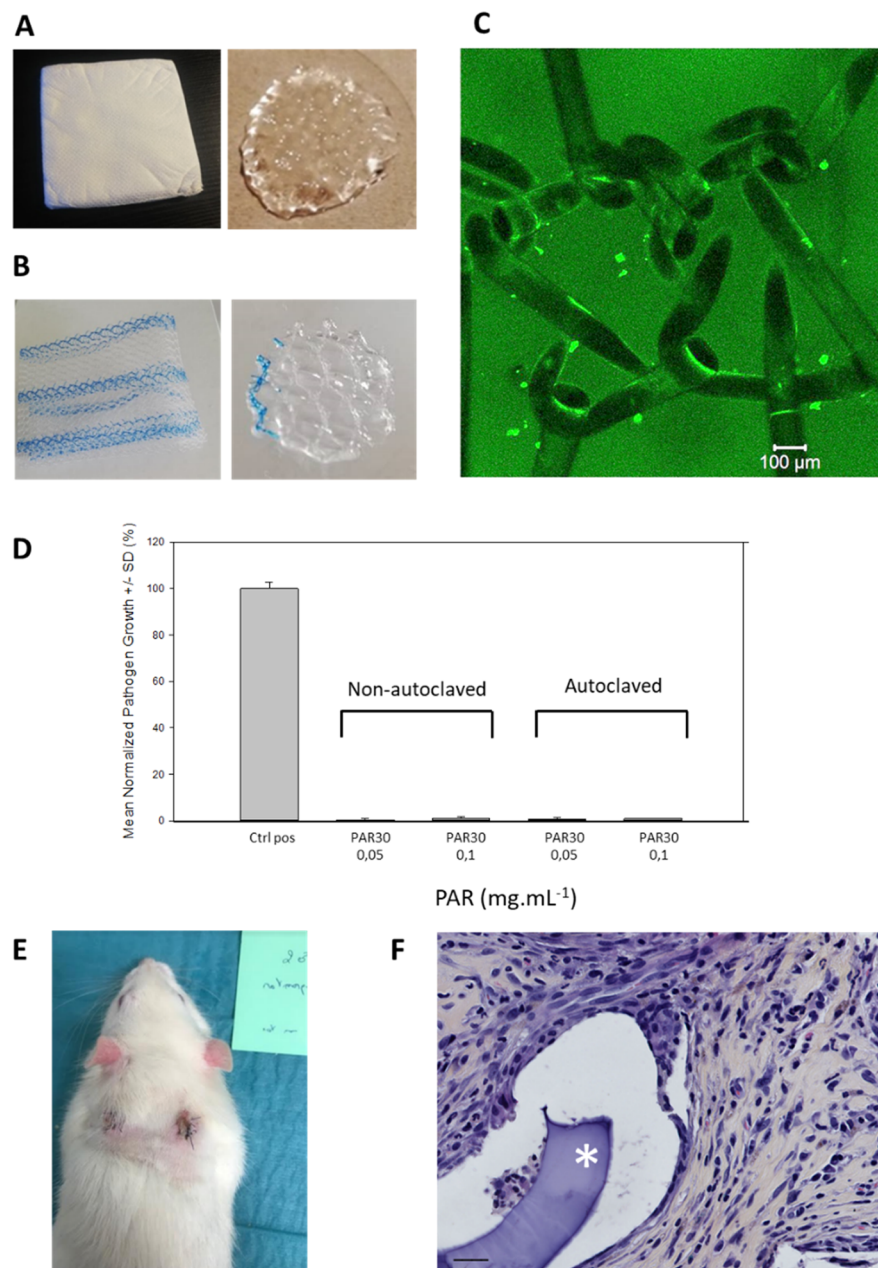
Figure 7. Deposition of HA hydrogels on medical devices. (A) Medicomp was cut into 12 mm diameter pieces and embedded with the HA hydrogel. (B) Gynecare Gynemesh was cut into 12 mm diameter pieces and embedded with the HA hydrogel. (C) Confocal microscopy image of PAR30-FITC-loaded HA hydrogels deposited onto Gynecare Gynemesh. (D) Effect of autoclaving on antibacterial activity of HA-PAR hydrogels. Hydrogels were deposited onto PP mesh prosthesis, loaded with 0.05 and 0.1 mg·mL^{-1} of PAR10 and PAR30 and autoclaved at 121 °C for 20 min. The graphs show bacterial growth in the presence of hydrogels after 24 h of incubation at 37 °C; 100% corresponds to a positive control (bacteria grown in absence of HA-PAR hydrogels). (E) Rat implantation sites. (F) Example of histological cross-sections of the explants showing the implanted hydrogel and the surrounding tissues. The hydrogel is marked by an asterisk.

deposited onto medical devices and allowing to control the release of antimicrobial agents. In this work, we introduced a unique and simple formulation of HA-based antimicrobial material. We developed negatively charged HA hydrogels which, via electrostatic interaction, can absorb high quantities of positively charged antimicrobial agent PAR. Such formulation provides a prolonged antibacterial effect in vitro because of the gradual release of PAR. Among three different tested PAR lengths, PAR with 30 residues (PAR30) showed the most prolonged antibacterial effect in a repetitive infection in vitro model, providing at least one-week of antibacterial

activity against Gram-positive *S. aureus*, the pathogen leading to multiple hospital-associated infections. HA-PAR30 hydrogels were also efficient against Gram-negative bacteria *E. coli* and *P. aeruginosa*.

The hydrogels can be tuned in terms of their size, quantities of loaded PAR, and their release kinetics. In addition, both PAR10 and PAR30-loaded antibacterial hydrogels with 2−4 days of antibacterial activity showed good in vitro biocompatibility. The hydrogels were successfully deposited on medical devices like fabrics or meshes used in clinical applications (Medicomp and Gynecare Gynemesh), and antibacterial

activity of the resulting constructs was preserved after drying and autoclaving, which is important for its potential use in clinics.

Finally, we performed first in vivo tests of hydrogel-coated mesh material biocompatibility in a rat model, which showed no difference between control HA hydrogel and PAR-loaded hydrogel. The next step of our work will be related to further in vivo studies of hydrogel biocompatibility, as well as their antibacterial activity in the infected model.

■ ASSOCIATED CONTENT

Ⓢ Supporting Information

The Supporting Information is available free of charge at https://pubs.acs.org/doi/10.1021/acsami.9b23140.

Antibacterial activity of HA hydrogels loaded with PAR: repetitive culture, schematic presentation of direct in vitro cytotoxicity test, loading of PAR30-FITC into HA hydrogel discs, antibacterial activity of HA hydrogel discs loaded with PAR: *S. aureus*, antibacterial activity of HA hydrogels loaded with PAR30: *E. coli* and *P. aeruginosa*, cytotoxicity assay with higher concentrations of PAR10 and PAR30, cytotoxicity assay after 24 and 48 h, antibacterial activity of hydrogel discs and hydrogel-coated meshes loaded with PAR, in vivo biocompatibility assessment: histological analysis, and macroscopic outcomes of the implants (PDF)

■ AUTHOR INFORMATION

Corresponding Author

Philippe Lavalle − *Institut National de la Santé et de la Recherche Médicale, INSERM Unité 1121 Biomaterials and Bioengineering, 67085 Strasbourg Cedex, France; Faculté de Chirurgie Dentaire, Université de Strasbourg, 67000 Strasbourg, France; SPARTHA Medical, 67000 Strasbourg, France;* ⓞ orcid.org/0000-0001-8798-912X; Phone: 33(0) 368853061; Email: philippe.lavalle@inserm.fr

Authors

Varvara Gribova − *Institut National de la Santé et de la Recherche Médicale, INSERM Unité 1121 Biomaterials and Bioengineering, 67085 Strasbourg Cedex, France; Faculté de Chirurgie Dentaire, Université de Strasbourg, 67000 Strasbourg, France*

Fouzia Boulmedais − *Institut Charles Sadron, CNRS UPR 22, 67034 Strasbourg, France;* ⓞ orcid.org/0000-0002-4934-9276

Agnès Dupret-Bories − *Institut Claudius Regaud, Institut Universitaire de Toulouse Oncopole, 31059 Toulouse Cedex 9, France*

Cynthia Calligaro − *Institut National de la Santé et de la Recherche Médicale, INSERM Unité 1121 Biomaterials and Bioengineering, 67085 Strasbourg Cedex, France; Faculté de Chirurgie Dentaire, Université de Strasbourg, 67000 Strasbourg, France*

Bernard Senger − *Institut National de la Santé et de la Recherche Médicale, INSERM Unité 1121 Biomaterials and Bioengineering, 67085 Strasbourg Cedex, France; Faculté de Chirurgie Dentaire, Université de Strasbourg, 67000 Strasbourg, France*

Nihal Engin Vrana − *SPARTHA Medical, 67000 Strasbourg, France*

Complete contact information is available at:

https://pubs.acs.org/10.1021/acsami.9b23140

Author Contributions

The manuscript was written through contributions of all the authors. All the authors have given approval to the final version of the manuscript.

Notes

The authors declare no competing financial interest.

■ ACKNOWLEDGMENTS

■ REFERENCES

(1) VanEpps, J. S.; Younger, J. G. Implantable Device-Related Infection. *Shock* 2016, 46, 597−608.

(2) Bayramov, D. F.; Neff, J. A. Beyond Conventional Antibiotics - New Directions for Combination Products to Combat Biofilm. *Adv. Drug Delivery Rev.* 2017, 112, 48−60.

(3) Römling, U.; Balsalobre, C. Biofilm Infections, Their Resilience to Therapy and Innovative Treatment Strategies. *J. Intern. Med.* 2012, 272, 541−561.

(4) Costerton, J. W.; Stewart, P. S.; Greenberg, E. P. Bacterial Biofilms: A Common Cause of Persistent Infections. *Science* 1999, 284, 1318−1322.

(5) von Eiff, C.; Jansen, B.; Kohnen, W.; Becker, K. Infections Associated with Medical Devices: Pathogenesis, Management and Prophylaxis. *Drugs* 2005, 65, 179−214.

(6) Darouiche, R. O. Antimicrobial Approaches for Preventing Infections Associated with Surgical Implants. *Clin. Infect. Dis.* 2003, 36, 1284−1289.

(7) Musella, M.; Guido, A.; Musella, S. Collagen Tampons as Aminoglycoside Carriers to Reduce Postoperative Infection Rate in Prosthetic Repair of Groin Hernias. *Eur. J. Surg.* 2001, 167, 130−132.

(8) van Vugt, T. A. G.; Walraven, J. M. B.; Geurts, J. A. P.; Arts, J. J. C. Antibiotic-Loaded Collagen Sponges in Clinical Treatment of Chronic Osteomyelitis. *J. Bone Jt. Surg., Am. Vol.* 2018, 100, 2153−2161.

(9) Westberg, M.; Frihagen, F.; Brun, O.-C.; Figved, W.; Grogaard, B.; Valland, H.; Wangen, H.; Snorrason, F. Effectiveness of Gentamicin-Containing Collagen Sponges for Prevention of Surgical Site Infection after Hip Arthroplasty: A Multicenter Randomized Trial. *Clin. Infect. Dis.* 2015, 60, 1752−1759.

(10) Pitarresi, G.; Palumbo, F. S.; Calascibetta, F.; Fiorica, C.; Di Stefano, M.; Giammona, G. Medicated Hydrogels of Hyaluronic Acid Derivatives for Use in Orthopedic Field. *Int. J. Pharm.* 2013, 449, 84−94.

(11) Hu, J.; Zheng, Z.; Liu, C.; Hu, Q.; Cai, X.; Xiao, J.; Cheng, Y. A Ph-Responsive Hydrogel with Potent Antibacterial Activity against Both Aerobic and Anaerobic Pathogens. *Biomater. Sci.* 2019, 7, 581−584.

(12) Li, B.; Webster, T. J. Bacteria Antibiotic Resistance: New Challenges and Opportunities for Implant-Associated Orthopedic Infections. *J. Orthop. Res.* 2018, 36, 22−32.

(13) Vasilev, K.; Cavallaro, A.; Zilm, P. Special Issue: Antibacterial Materials and Coatings. *Molecules* 2018, 23, 585−588.

(14) AshaRani, P. V.; Low Kah Mun, G.; Hande, M. P.; Valiyaveettil, S. Cytotoxicity and Genotoxicity of Silver Nanoparticles in Human Cells. *ACS Nano* 2009, 3, 279−290.

(15) Mahlapuu, M.; Hakansson, J.; Ringstad, L.; Bjorn, C. Antimicrobial Peptides: An Emerging Category of Therapeutic Agents. *Front. Cell. Infect. Microbiol.* **2016**, *6*, 194−205.

(16) Yu, Y.; Yang, Z.; Ren, S.; Gao, Y.; Zheng, L. Multifunctional Hydrogel Based on Ionic Liquid with Antibacterial Performance. *J. Mol. Liq.* **2020**, *299*, 112185−112192.

(17) Wu, D.-Q.; Zhu, J.; Han, H.; Zhang, J.-Z.; Wu, F.-F.; Qin, X.-H.; Yu, J.-Y. Synthesis and Characterization of Arginine-Nipaam Hybrid Hydrogel as Wound Dressing: In Vitro and in Vivo Study. *Acta Biomater.* **2018**, *65*, 305−316.

(18) Chang, K.-C.; Lin, D.-J.; Wu, Y.-R.; Chang, C.-W.; Chen, C.-H.; Ko, C.-L.; Chen, W.-C. Characterization of Genipin-Crosslinked Gelatin/Hyaluronic Acid-Based Hydrogel Membranes and Loaded with Hinokitiol: In Vitro Evaluation of Antibacterial Activity and Biocompatibility. *Mater. Sci. Eng., C* **2019**, *105*, 110074−110082.

(19) Qu, J.; Zhao, X.; Liang, Y.; Zhang, T.; Ma, P. X.; Guo, B. Antibacterial Adhesive Injectable Hydrogels with Rapid Self-Healing, Extensibility and Compressibility as Wound Dressing for Joints Skin Wound Healing. *Biomaterials* **2018**, *183*, 185−199.

(20) Li, S.; Dong, S.; Xu, W.; Tu, S.; Yan, L.; Zhao, C.; Ding, J.; Chen, X. Antibacterial Hydrogels. *Adv. Sci.* **2018**, *5*, 1700527−1700543.

(21) Ng, V. W. L.; Chan, J. M. W.; Sardon, H.; Ono, R. J.; García, J. M.; Yang, Y. Y.; Hedrick, J. L. Antimicrobial Hydrogels: A New Weapon in the Arsenal against Multidrug-Resistant Infections. *Adv. Drug Delivery Rev.* **2014**, *78*, 46−62.

(22) Yang, K.; Han, Q.; Chen, B.; Zheng, Y.; Zhang, K.; Li, Q.; Wang, J. Antimicrobial Hydrogels: Promising Materials for Medical Application. *Int. J. Nanomed.* **2018**, *13*, 2217−2263.

(23) Mutschler, A.; Tallet, L.; Rabineau, M.; Dollinger, C.; Metz-Boutigue, M.-H.; Schneider, F.; Senger, B.; Vrana, N. E.; Schaaf, P.; Lavalle, P. Unexpected Bactericidal Activity of Poly(Arginine)/Hyaluronan Nanolayered Coatings. *Chem. Mater.* **2016**, *28*, 8700−8709.

(24) Decher, G. Fuzzy Nanoassemblies: Toward Layered Polymeric Multicomposites. *Science* **1997**, *277*, 1232−1237.

(25) Özçelik, H.; Vrana, N. E.; Gudima, A.; Riabov, V.; Gratchev, A.; Haikel, Y.; Metz-Boutigue, M.-H.; Carradò, A.; Faerber, J.; Roland, T.; Klüter, H.; Kzhyshkowska, J.; Schaaf, P.; Lavalle, P. Harnessing the Multifunctionality in Nature: A Bioactive Agent Release System with Self-Antimicrobial and Immunomodulatory Properties. *Adv. Healthcare Mater.* **2015**, *4*, 2026−2036.

(26) Mutschler, A.; Betscha, C.; Ball, V.; Senger, B.; Vrana, N. E.; Boulmedais, F.; Schroder, A.; Schaaf, P.; Lavalle, P. Nature of the Polyanion Governs the Antimicrobial Properties of Poly(Arginine)/Polyanion Multilayer Films. *Chem. Mater.* **2017**, *29*, 3195−3201.

(27) Almond, A. Hyaluronan. *Cell. Mol. Life Sci.* **2007**, *64*, 1591−1596.

(28) Dicker, K. T.; Gurski, L. A.; Pradhan-Bhatt, S.; Witt, R. L.; Farach-Carson, M. C.; Jia, X. Hyaluronan: A Simple Polysaccharide with Diverse Biological Functions. *Acta Biomater.* **2014**, *10*, 1558−1570.

(29) Fakhari, A.; Berkland, C. Applications and Emerging Trends of Hyaluronic Acid in Tissue Engineering, as a Dermal Filler and in Osteoarthritis Treatment. *Acta Biomater.* **2013**, *9*, 7081−7092.

(30) Pavesio, A.; Renier, D.; Cassinelli, C.; Morra, M. Anti-Adhesive Surfaces through Hyaluronan Coatings. *Med. Device Technol.* **1997**, *8*, 20−24.

(31) Ardizzoni, A.; Neglia, R. G.; Baschieri, M. C.; Cermelli, C.; Caratozzolo, M.; Righi, E.; Palmieri, B.; Blasi, E. Influence of Hyaluronic Acid on Bacterial and Fungal Species, Including Clinically Relevant Opportunistic Pathogens. *J. Mater. Sci.: Mater. Med.* **2011**, *22*, 2329−2338.

(32) Romanò, C. L.; De Vecchi, E.; Bortolin, M.; Morelli, I.; Drago, L. Hyaluronic Acid and Its Composites as a Local Antimicrobial/Antiadhesive Barrier. *J. Bone Joint Infect.* **2017**, *2*, 63−72.

(33) Lequeux, I.; Ducasse, E.; Jouenne, T.; Thebault, P. Addition of Antimicrobial Properties to Hyaluronic Acid by Grafting of Antimicrobial Peptide. *Eur. Polym. J.* **2014**, *51*, 182−190.

(34) Khunmanee, S.; Jeong, Y.; Park, H. Crosslinking Method of Hyaluronic-Based Hydrogel for Biomedical Applications. *J. Tissue Eng.* **2017**, *8*, 2041731417726464.

(35) Fidalgo, J.; Deglesne, P. A.; Arroyo, R.; Sepúlveda, L.; Ranneva, E.; Deprez, P. Detection of a New Reaction by-Product in Bdde Cross-Linked Autoclaved Hyaluronic Acid Hydrogels by Lc-Ms Analysis. *Med. Dev.* **2018**, *11*, 367−376.

(36) De Boulle, K.; Glogau, R.; Kono, T.; Nathan, M.; Tezel, A.; Roca-Martinez, J.-X.; Paliwal, S.; Stroumpoulis, D. A Review of the Metabolism of 1,4-Butanediol Diglycidyl Ether-Crosslinked Hyaluronic Acid Dermal Fillers. *Dermatol. Surg.* **2013**, *39*, 1758−1766.

(37) Grant, S. S.; Hung, D. T. Persistent Bacterial Infections, Antibiotic Tolerance, and the Oxidative Stress Response. *Virulence* **2013**, *4*, 273−283.

(38) Arnold, M. R.; Kao, A. M.; Gbozah, K. K.; Heniford, B. T.; Augenstein, V. A. Optimal Management of Mesh Infection: Evidence and Treatment Options. *Int. J. Abdom. Wall Hernia Surg.* **2018**, *1*, 42−49.

(39) Wang, X. H.; Li, D. P.; Wang, W. J.; Feng, Q. L.; Cui, F. Z.; Xu, Y. X.; Song, X. H.; van der Werf, M. Crosslinked Collagen/Chitosan Matrix for Artificial Livers. *Biomaterials* **2003**, *24*, 3213−3220.

(40) Duarte, M. L.; Ferreira, M. C.; Marvão, M. R.; Rocha, J. An Optimised Method to Determine the Degree of Acetylation of Chitin and Chitosan by Ftir Spectroscopy. *Int. J. Biol. Macromol.* **2002**, *31*, 1−8.

(41) Haxaire, K.; Maréchal, Y.; Milas, M.; Rinaudo, M. Hydration of Polysaccharide Hyaluronan Observed by Ir Spectrometry. I. Preliminary Experiments and Band Assignments. *Biopolymers* **2003**, *72*, 10−20.

(42) De Maria, C.; Santoro, V.; Vozzi, G. Biomechanical, Topological and Chemical Features That Influence the Implant Success of an Urogynecological Mesh: A Review. *BioMed Res. Int.* **2016**, *2016*, 1267521.